Ion Winds in Saturn's southern auroral/polar region

Tom S. Stallard[1,2], Steve Miller[1,2], Laurence M. Trafton[3], Thomas R. Geballe[4] and Robert D. Joseph[5]

[1] Department of Physics and Astronomy, University College London, Gower Street, London WC1 6BT, U.K.

[2] Visiting astronomer at the Infrared Telescope Facility, which is managed for NASA by the University of Hawaii Institute for Astronomy.

[3] McDonald Observatory, University of Texas at Austin, Austin, Texas 78712, U.S.A.

[4] Gemini Observatory, 670 N. A'ohoku Place, Hilo, Hawaii 96720, U.S.A.

[5] Institute for Astronomy, Woodlawn Drive, Honolulu, Hawaii 96822, U.S.A.

Abstract

We present profiles of the line-of-sight (l.o.s.) ionospheric wind velocities in the southern auroral/polar region of Saturn. Our velocities are derived from the measurement of Doppler shifting of the H_3^+ ν_2 Q(1,0$^-$) line at 3.953 microns. The data for this study were obtained using the facility high-resolution spectrometer CSHELL on the NASA Infrared Telescope Facility (IRTF) on Mauna Kea, Hawaii, during the night of February 6, 2003 (UT). The l.o.s. velocity profiles finally derived are consistent with an extended region of the upper atmosphere sub-corotating with the planet: the ion velocities in the inertial reference are only 1/3 of those expected for full planetary corotation. We discuss the results in the light of recent proposals for the kronian magnetosphere, and suggest that, in this region, Saturn's ion winds may be under solar wind control.

Introduction

Auroral emission from Saturn's polar regions was first detected by the Pioneer 11 spacecraft (Judge *et al.*, 1980). Since then, there have been observations in the ultraviolet by the International Ultraviolet Explorer (Clarke *et al.*, 1981), Voyager (Sandel and Broadfoot, 1981) and – most recently – the Hubble Space Telescope (e.g. Trauger *et al.*, 1998). At the time of the Voyager encounter, Saturn's UV auroral emission was ~3% of that of Jupiter (Broadfoot *et al.*, 1981). Saturn has been known to produce infrared emission from the H_3^+ molecular ion since 1993 (Geballe *et al.*, 1993), which is approximately two orders of magnitude weaker than that from Jupiter (even weaker than uranian H_3^+ emission). More recently, this infrared emission was shown to be (mainly) auroral in nature (Stallard *et al.*, 1999), rather than due to a planetwide "glow", as is the case for Uranus (Trafton *et al.*, 1999).

Our understanding of how Jupiter produces its auroral emission has developed over the last few years with the renewed interest in the theory first developed by Hill in the late 1970s (Hill, 1979; Hill and Dessler, 1991). In particular, Hill himself (2001) and Cowley and Bunce (2001) demonstrated that the main, bright jovian auroral oval corresponded to powerful field-aligned currents generated in the middle magnetosphere, where the equatorial plasmasheet starts to lag behind corotation with the planet. As the plasmatubes associated with the jovian magnetic field are slowed by the plasmasheet, the Hill/Cowley/Bunce (HCB)

model predicts that a powerful equatorward electric field should be generated in the jovian ionosphere, across the auroral oval. This, in turn, combining with the planetary magnetic field, should drive an ion wind around the auroral oval, clockwise as viewed from above the north pole and anti-clockwise from above the south; in both hemispheres, the ion wind should be against the rotation of the planet. Such winds were first detected by Rego and co-workers in 1999 (Rego *et al.*, 1999). Subsequent work by Stallard and co-workers showed that this "electrojet" flowed continuously, with velocities in the line-of-sight between ~0.5 km/s and 1.5 km/s (Stallard *et al.*, 2001: henceforth Paper I). Paper I also showed that there was a region poleward of the auroral oval, that these authors termed the Dark Polar Region (DPR), which showed a strong anti-sunward flow, when viewed in the frame of reference rotating with the planet (henceforth the Planetary Reference Frame). Further work (Cowley *et al.*, 2003a; Stallard *et al*. 2003) showed that this DPR corresponded to a region of (near-)stagnation viewed in the frame of reference of the jovian magnetic pole. This was typical of a region corresponding to the footprints of open field lines, under solar wind control and swept back into the magnetotail, similar to the Earth's polar cap.

The new interpretations of the situation for Jupiter naturally raised the question of what to expect for Saturn, particularly in the run up to the arrival of Cassini/Huygens at the kronian system in 2004. Cowley and co-workers have revisted kronian magnetospheric models (Cowley *et al.*, 2003b; henceforth Paper II) in the light of recent images of the auroral oval from the STIS instrument on

the HST and Voyager measurements of magnetospheric plasma flow at Saturn. They conclude that an HCB mechanism cannot be responsible for the bright auroral oval, since it produces too little precipitation for the case of Saturn. Instead, they propose that the oval marks the junction between the footprints of closed field lines, on which ionospheric ions should move at velocities 60% to 80% of the rigid planetary corotation, and open field lines, connecting to the magnetotail, which should show a significant additional lag behind corotation. The prediction of Paper II is that ionospheric ion-neutral collisions should be able to drag the ions attached to open field lines into ~25% of corotation.

Independent of Cowley and co-workers, we had proposed to extend the techniques developed for Jupiter to Saturn. This paper presents the first ever measurements of ion winds on Saturn, and compares them with the predictions of Paper II.

Observations

This paper is based on observations of the auroral/polar region of Saturn carried out on February 6, 2003, using the high resolution facility spectrometer CSHELL on the NASA Infrared Telescope Facility (IRTF) on Mauna Kea, Hawaii (Greene *et al.*, 1993). At that time, Saturn's equatorial diameter subtended 19.7" on the sky, and the sub-Earth latitude was -32^{o}. For the latter reason, only the southern auroral/polar region could be observed, the north being obscured by the rings.

For our observations, which are tabulated in Table I, we set the CSHELL slit parallel to the planetary equator and located so as to cut across the auroral oval at the ansa. We measured the H_3^+ ν_2 Q(1,0$^-$) line at 3.953 microns, using the highest spectral resolution available, $\lambda/\Delta\lambda$ ~40,000, to look for Doppler shifting of the line. Much of the observational technique required is based on our observations of Jupiter, and given in Paper I. So we concentrate here on the main differences, which stem from the fact that the kronian auroral emission intensity is ~1% of the equivalent jovian emission.

There are two main consequences of the lower intensity:

- It is not possible to obtain H_3^+ images, even using the Connerney-Satoh filter, in any exposure period of reasonable length (i.e. less than 3 hours);
- Exposure times for kronian H_3^+ spectroscopy have to be much longer than for Jupiter, where typically 60 s is sufficient to get signal-to-noise (S/N) ratios ~50-100 on CSHELL.

The impact of the first consequence will be discussed later. The impact of the second is that guiding the telescope on the planet is extremely important, if one wishes to obtain spectral information about a particular location. This is vital since the velocity measured in the line-of-sight may vary from position to position across the auroral/polar region. With the high-resolution set-up selected for these observations, one pixel spanned 0.2” along the CSHELL slit, and 0.5” perpendicular to it. Seeing on February 6, 2003, was ~0.6” or better. Thus the

main problems in terms of accurately locating the slit on the planet were due to the limits on the ability of the IRTF to track Saturn, and to point back to the same place after the necessary offsets to observe blank sky for sky-subtraction purposes.

For a point source, the telescope's own guidance system can ensure that this is effected with a high degree of accuracy. Unfortunately, an object as extended as Saturn is too large for the guidance system to handle. Thus accurate guiding had to be achieved in two ways:

- The pointing was continually manually adjusted by the observer (using a software-generated control "paddle") by reference to a planetary-ring outline drawn on the guidance monitor;
- The "Saturn track rate" (its differential rate compared with the pre-programmed sidereal track rate) was manually updated by the telescope operator at regular intervals during observation as a result of input from the observer.

Both of these techniques required intense concentration of a kind that is difficult to sustain at the ~4,000m altitude of the IRTF control room for long periods of time. This effectively limited exposure times for individual runs to little more than 1 hour elapse time. Typically, this was made up of 7.5 quads consisting of: a 120 s individual exposure on the planet, followed by two 120 s on blank sky, followed

by a further on-planet exposure ('ABBA' mode, see Table 1). This series of exposures was co-added to increase S/N.

Such long exposures clearly mean that our results represent averages for Saturn's auroral/polar regions. This would produce results for Jupiter, for which the exact location of the auroral oval is extremely dependent on longitude, that would be very hard to interpret. For Saturn, brightness modulations have been recorded on timescales comparable to our exposures (Gurnett *et al.*, 1981; Kaiser *et al.*, 1984; J.-C. Gérard, private communication), and there are clear local time effects visible in the best quality UV images available (Paper II). However, the rotational and magnetic poles coincide, making it likely that the spatial location of the auroral oval will be relatively independent of longitude (J.-C. Gérard, private communication). Thus, in the absence of longitudinal effects that cause spatial smearing of the auroral geometry, long exposures are able to produce worthwhile average information for Saturn.

Spectral image and intensity profile

In Fig. 1 we present a sky-subtracted spectral image of Saturn in the region 3.9479 to 3.9581 microns, centred on the 3.953μm Q(1,0$^-$) H_3^+ line. The y-axis corresponds to wavelength, and the x-axis to east-west on the sky (left-right) spatial extension across the planet. The spectral image is the result of co-adding all the data obtained on February 6, 2003, effectively a 5400 s exposure on the

planet minus the same amount on blank sky. This spectral image was made up of three separate runs, each consisting of a total exposure time of 1800 s (see Table I). The spectral image has been corrected for array distortion as explained in Paper I, and thus is a good spectral/spatial representation of Saturn's behaviour at these wavelengths.

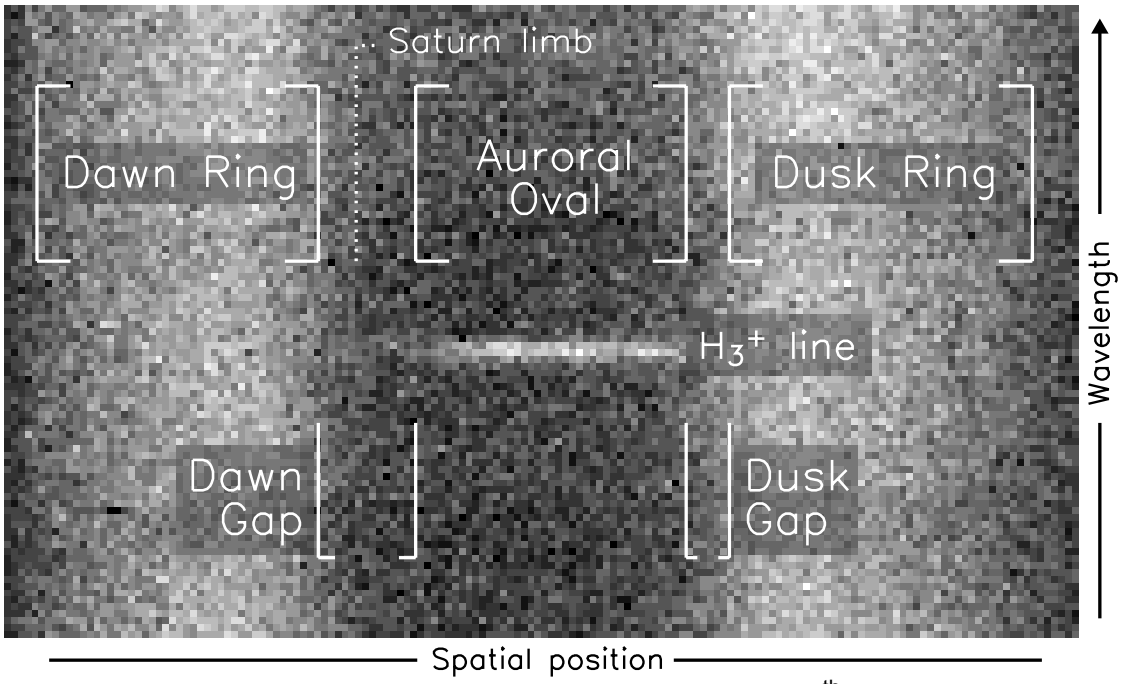

Figure 1 - The integrated spectral image of Saturn from 6th February 2003, with wavelength variation on the y-axis, and the E-W spatial variation on the x-axis. East on the sky is left on the figure; west on the sky is right.

Table I: Observations

UT Date and Time	Seq. Name	No. of AB frames	CML	Airmass
6 Feb. 06:53	06Feb#1	15	232.1	1.001
6 Feb. 08:57	06Feb#2	15	302.0	1.166
6 Feb. 10:13	06Feb#3	15	344.7	1.520

The planet's spectrum is characterised by a dark central region (along the spatial x-axis) with some bright bands at the shorter wavelength end of the spectral region covered and some faint bands at longer wavelengths. These are typical of reflected solar radiation plus planetary infrared continuum emission from the lower atmosphere that is only partially absorbed by methane in the kronian stratosphere (see Stallard *et al.*, 1999). East (left) and west (right) of the planet is the continuum spectrum of sunlight reflected from the rings. In the centre of the spectral image is a bright, narrow (in the spectral y-axis) emission line set against an almost-zero continuum level. This is the 3.953μm $Q(1,0^-)$ H_3^+ line, and at its brightest the line is visible with a S/N ratio of 20. It can be seen extending across the planet, merging slightly into the ring continuum in the west.

In Fig. 2 we show the east-west intensity profile of the spectral image produced by each of our three runs on February 6, as well as that of the summed image shown in Fig. 1. The H_3^+ intensity profile (solid line) is produced by fitting the line profile at each spatial position to a gaussian, taking the (rolling) average intensity over 5 pixels to improve the S/N, and then plotting the peak intensity. This is a smoothing over 1", which is equivalent to ~6000 km at Saturn. This smooting enables the low-level continuum intensity to be accurately subtracted from the line intensity, even where the line begins to blend with the ring spectrum in the west. The ring continuum intensity (dashed line) is produced by summing each spatial position across the entire wavelength range (3.9479-3.9581μm), and then normalising to show it on the same intensity scale as the H_3^+ line.

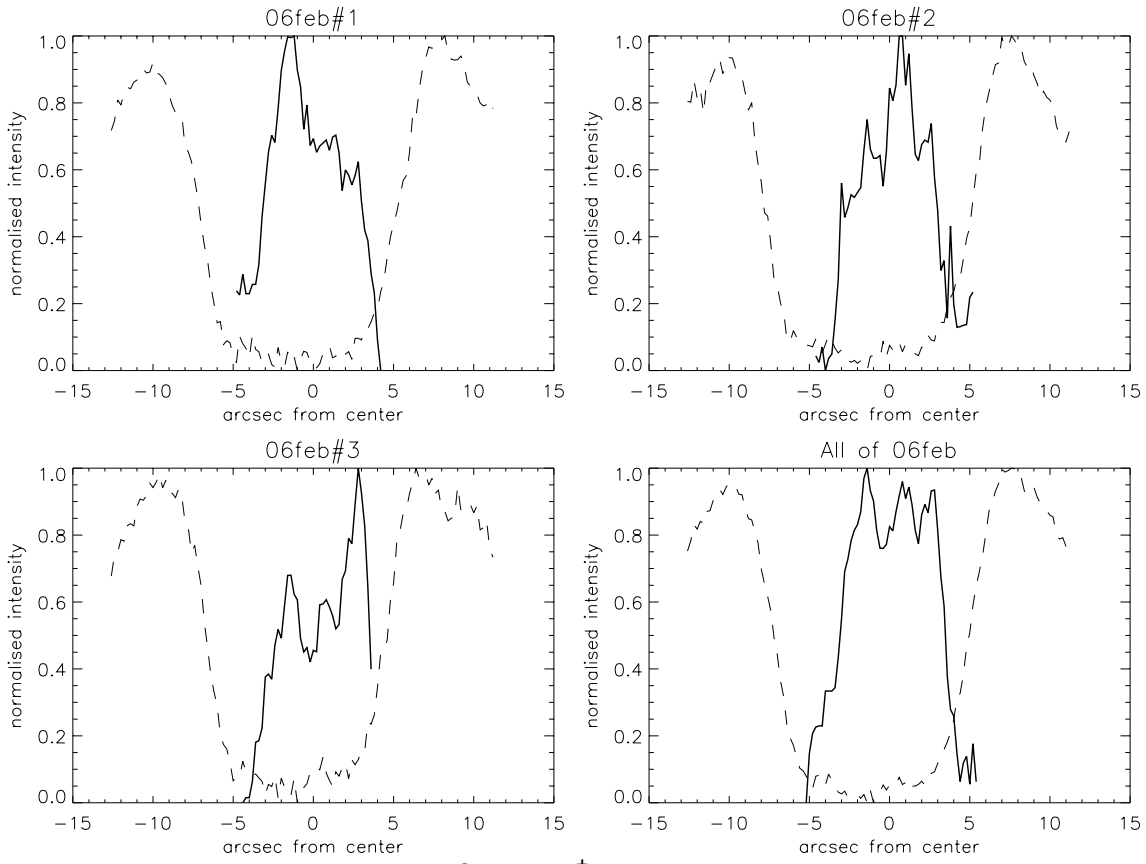

Figure 2a-d – The normalised fitted H_3^+ intensities, plotted with the combined reflected ring continuum. The first three plots, a-c, show the results for the individual sets of integration, while the final plot, d, shows the product of these.

UV emission from Saturn's auroral/polar regions shows a narrow, bright oval, particularly in the dawnside (east on the sky), although the setting oval is more diffuse (Trauger *et al.*, 1998; Paper II). Poleward of the UV oval the planet has little emission, although occasional bright features are seen. In contrast, Figs. 1 and 2 show that there is H_3^+ emission across the entire auroral/polar region, using an east-west slit configuration. In this respect, Saturn is similar to Jupiter, for which a corresponding contrast between UV and H_3^+ emission has been

noted (Paper I). It is possible that Figs. 1 and 2 demonstrate smearing of a bright auroral oval as a result of poor seeing and pointing errors. The following section, however, shows that this is unlikely to be the case.

Analysis of intensity profiles

In order to analyse Fig. 2, it is helpful to look at the predicted configuration of Saturn for February 6, 2003. This is shown in Fig. 3, based on the predictions of the Planetary Data System 'Planet Viewer' (http://ringside.arc.nasa.gov). Onto this figure we have superimposed a cylindrical approximation of the observed auroral oval of Cowley *et al*. (2003b), degraded to the 1" smoothing we have used in Fig. 2, and assuming (for visualisation purposes) that the auroral intensity is constant around the oval. To the nearest arcsecond, the (smeared) auroral oval extends 7" across the planet from dawnside-to-duskside at its maximum extent – we label this the Oval. The planet casts a shadow on the easterly (in the observer's reference frame) rings of ~2-3" at the latitude of the southern auroral oval ansa. This means that from east to west, there is a gap of ~11-12" between the (illuminated) rings – we label this the Ring-to-Ring Gap (R-R Gap, for short). In the east (dawnside) there is a gap of 3-4" between the dawn auroral ansa and the illuminated ring – we label this the Dawn Gap; in the west (duskside) this is 1" – the Dusk Gap. Figure 3 therefore gives us constraints in estimating the potential spatial smearing of our results, due to seeing and pointing errors, as well as an estimate of our location on the planet.

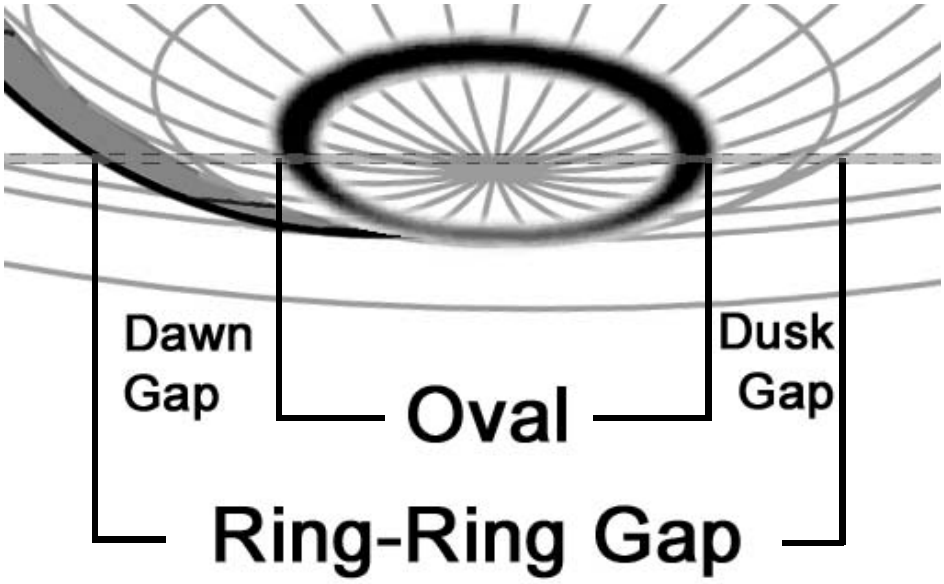

Figure 3 – The hypothesised auroral oval plotted oval the planetary configuration at the time of observations, including the shadow of the planet on the rings. The E-W position of the slit is marked by the narrow dashed box, latitude is marked in 15° increments, and the diagram is representative and not fully to scale.

In Fig. 2d, we have measured the dimensions of the features outlined above for Fig. 3, at the half-intensity of the ring continuum. The results for these, given in Table II, compare well with those predicted from Fig. 3, and indicate that the spectral image was obtained with the slit close to cutting the auroral ansas and that our efforts to maintain position on the planet during the course of the observations were successful.

Table II: Intensity profiles for Feb. 6

	Oval	R-R Gap	Dawn Gap	Dusk Gap
Predicted	**7”**	**11” - 12”**	**3” - 4”**	**1”**
06Feb all	6.6”	11.8”	4”	1.2”
06Feb#1	6.6”	11.8”	3.6”	1.6”
06Feb#2	6.2”	12.4”	4.4”	1.8”
06Feb#3	5.8”	10.8”	4.4”	0.6”

Some indication of the variation in the results obtained is shown in Fig. 2a-c, where the intensity profiles for the three component runs making up Figs. 1 and 2d are shown. Analysis of these three, in terms of the features noted in Fig. 3 are also presented in Table II. These indicate that 06Feb#1 was probably closely aligned across the auroral ansas. But 06Feb#2, with its smaller than expected Oval and larger than expected R-R Gap may have been aligned slightly too far north on the sky. Conversely, 06Feb#3, with its smaller than expected Oval and smaller than expected R-R Gap, may have been aligned too far south. Nonetheless, all three runs have the slit crossing very close to the auroral ansas, and cutting the southern pole.

Attempts to produce the intensity profile seen in Fig. 2 by modelling the configuration shown in Fig. 3 smeared due to seeing and pointing errors still produced a double peaked structure, with a strong central minimum in the middle of the polar region, even when the unrealistically large smearing value of +/-2” was used. We therefore consider that these measurements could not result from bad seeing and large pointing errors, and that – like Jupiter – Saturn does have considerable polar H_3^+ emission.

Velocity profiles

Velocity profiles in the observer's line-of-sight (l.o.s.) across the planet for the night of February 6, 2003, are presented in Fig. 4, for the three individual runs (Figs. 4a-c) and for the composite spectral image (Fig. 4d). The l.o.s. velocities (henceforth simply "velocities") are (as with the intensities) rolling averages of five pixel peak wavelength positions resulting from the gaussian fitting procedure. They have been subject to array distortion correction, but – in contrast to Paper I – we have not transformed them to the Planetary Reference Frame by removing the rotational velocity of the planet in the l.o.s. Nor has it been possible to carry out a spatial correction for any effect of uneven illumination across the slit, since it was not possible to obtain H_3^+ images. We would argue, however, that in the case of Saturn, such spatial corrections as there might be are rather small, due to the axi-symmetric nature of the kronian magnetic field, with respect to the rotational axis, and the fact that we have chosen the smallest slit available on CSHELL in order to minimise such effects. Nonetheless, at this stage of our study of Saturn's auroral polar wind system, we choose to concentrate on average behaviour, rather than the more detailed spatial analysis that it proved possible to carry out for Jupiter (Paper I).

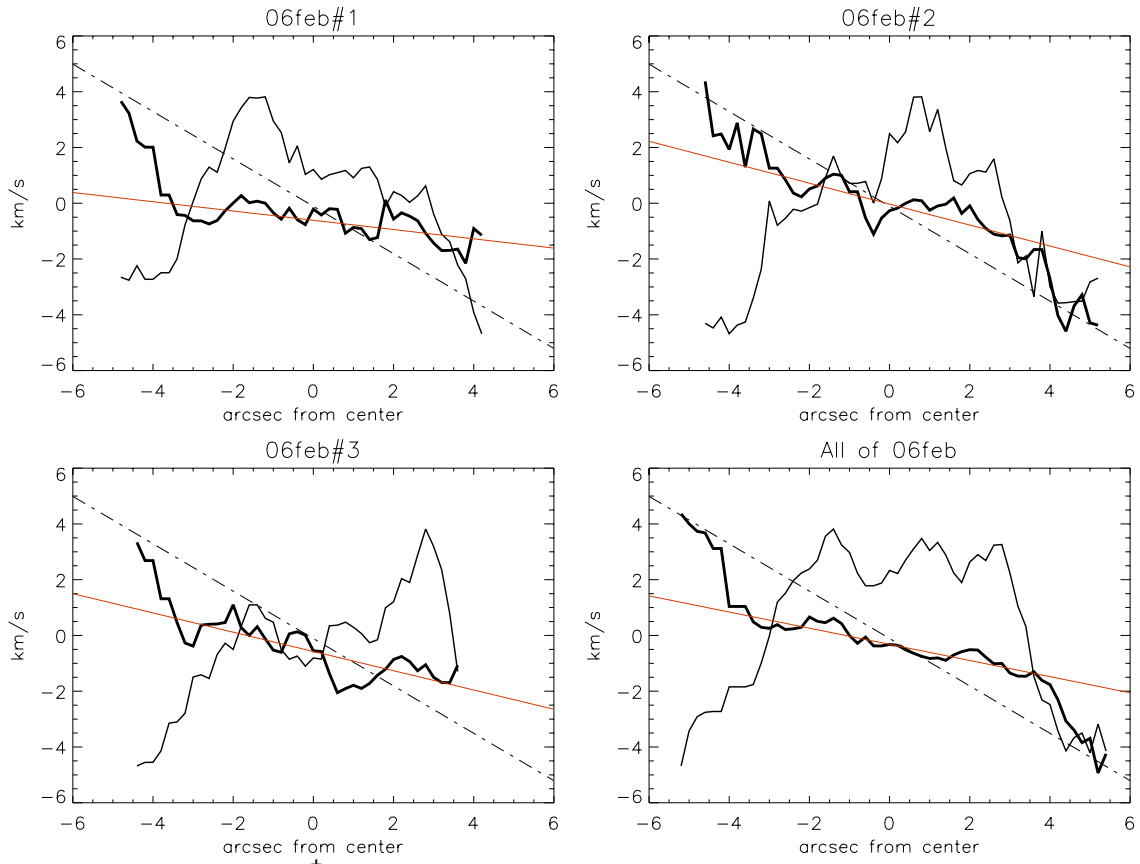

Figure 4a-d – The H_3^+ velocity structure across the auroral region, placed in an inertial frame, with the predicted velocity of a fully corotating atmosphere, and the fitted slope of sub-corotation across the main oval. These are plotted against the normalised H_3^+ intensity, as shown in Fig.2a-d.

In Fig. 4, we have overplotted the velocity profile with the H_3^+ intensity profiles to aid visualisation. Arbitrarily, we initially chose the centre of the planet to have zero velocity, although it turns out – in what follows - that this was a good choice. Once more to aid visualisation, we have overplotted the velocity corresponding to complete corotation with the planet (dot-dashed line, allowing for the sub-Earth latitude of Saturn at the time of observation). The measured velocity profiles for the auroral/polar region show much less spatial variation than was the case for

Jupiter (Paper I). In particular, there does not appear to be the strong blue-shifted Setting Auroral Oval (SAO)/red-shifted Rising Auroral Oval (RAO) structure that typified the jovian auroral electrojet. Instead, the velocity profile across the auroral/polar region seems rather uniformly sub-corotational across the auroral/polar region, a feature that is emphasised by our fitting of a straight line (dotted) through the velocities obtained.

Overall, Fig. 4d shows that our results have the auroral/polar regional velocity to be ~34% corotational, with the individual profiles at 20%, 44% and 40% for runs 06Feb#1, 06Feb#2 and 06Feb#3 respectively. It is also noteworthy that – given our decision to arbitrarily assign zero velocity to the centre of the planet – the velocities outside of the auroral/polar region, on the body of the planet at sub-auroral latitudes, return to corotational, as will be explained below.

A new model of Saturn's polar ionospheric flows

Paper II proposes a new model for the plasma flows in the kronian ionosphere based on considerations of the electron precipitation and currents required to power the main auroral oval, and its location. The picture presented is one in which the oval maps to the boundary between sub-auroral ionospheric plasma, which is tied onto closed field lines, and auroral/polar cap ionospheric plasma, tied to open field lines. (This is in contrast to the jovian main auroral oval, which is produced at the boundary between closed field lines that map into the

corotating equatorial plasmasheet and closed field lines that map that region where corotation is breaking down significantly.) Paper II suggests that in those regions which include and are poleward of the kronian auroral oval, the ionospheric plasma will lag significantly behind corotation with the planet, due to the way in which the solar wind sweeps open field lines slowly down-tail. Equatorward of the oval, however, the ionospheric plasma on closed field lines should rotate much closer to corotation, since the drag of Saturn's equatorial plasmasheet is much less than that of Jupiter's (Richardson and Sittler, 1990). Paper II demonstrates that the boundary between these two ionospheric plasma regimes corresponds to a region of upward flowing current, and downward flowing, accelerated electrons, with the energy required to power the auroral oval. Our measurement of an average 34% corotational velocity for the H_3^+ ions in the auroral/polar region, made independently of Cowley and co-workers, strongly supports this aspect of Paper II's model. The return of the H_3^+ velocity towards corotation on the body of the planet, equatorward of the oval, is also in accord with this picture.

In addition to the lag behind corotation of the polar cap ionosphere, Paper II's model also deals with the mapping of the Dungey (1961) cycle and Vasyliunas (1983) X-lines onto the ionosphere. Paper II estimates that the flow velocities associated with Dungey cycle are ~200m s^{-1}, sunward in a narrow region near the dawn auroral oval, and anti-sunward across most of the polar cap. On the basis of the corotation lag producing an ion velocity of 550m s^{-1}, the combined

flow would be anti-sunward at ~750m s^{-1} at the dusk edge of the polar cap, and sunward at ~350m s^{-1}, at the dawn, with some structure in the flows in between. At the level of analyis of our data - which has been smoothed over 1" (~6000 km at Saturn) – presented here, we are not able to pick out the fine structure of the flow patterns predicted by Paper II, particularly in the region of the dawn oval, where the velocity commences to return to corotation. Instead, it is most probable the effects of the Dungey and Vasyliunas processes would show up as an antisunward (negative) shift in the zero position of the centre-of-cap velocity of ~200m s^{-1}, based on the figures quoted from Paper II above. Unfortunately, however, the lamp lines used to calibrate the CSHELL array do not enable us to reach this level of *absolute* accuracy in the determining the zero velocity position, although the *relative* velocity from pixel to pixel is well constrained. Thus we are currently unable to make any statement about the validity of the Dungey cycle and Vasyliunas flows predicted in Paper II.

Paper II predicts that the auroral/polar plasma angular velocity, resulting from the lag to corotation in the polar cap, should be given by:

$$\Omega = \Omega_S \, \mu_0 \Sigma^*_P \, V_{SW} / [1 + \mu_0 \Sigma^*_P \, V_{SW}] \qquad 1)$$

where:

Ω is the auroral/polar ionospheric plasma angular velocity

Ω_S is the angular velocity of Saturn

μ_0 is the permitivity of free space

Σ^*_P is the ionospheric Pedersen conductivity in the frame of reference of the neutral atmosphere, and

V_{SW} is the velocity of the solar wind at Saturn.

The discussion in Paper II shows that for a value of Σ^*_P of 0.5mho and V_{SW} = 500 km/s, Ω should be 0.24 Ω_S. Paper II also discusses the relation between Ω and the length of the magnetotail. For $\Omega = 0.24\ \Omega_S$, it estimates that ~50 hours are required for field lines that map to the magnetopause to flow to the tail centre and reconnect. The corresponding tail is ~1500R_S (kronian radii; 1R_s = 60,268 km). Equation 1 can be inverted to give:

$$\Sigma^*_P = \mu_0 V_{SW} \Omega / [\Omega_S - \Omega] \qquad 2)$$

Assuming the Paper II value for V_{SW} (= 500 km/s) and our value of $\Omega = 0.34\ \Omega_S$, produces Σ^*_P = 0.82mho. This would, in turn, correspond to ~31 hours during which the magnetic field line remains open, and a magnetotail that is ~1060R_s long, for the same value of the solar wind velocity.

It is possible to make estimates of the flux of precipitating electrons required to produce Σ^*_P = 0.82mho from the JIM global circulation model used to simulate Jupiter (Achilleos *et al*., 1998), if we assume that the jovian and kronian upper atmospheres behave similarly. Recent calculations by Millward *et al*. (2002) show

that >100mW m^{-2} of 10 keV electrons would be needed to produce this conductivity in the jovian atmosphere, significantly more than the values of 5-50mWm^{-2} proposed by Paper II on the basis of the observed UV emission. However, Millward *et al*. (2002) also demonstrate that the conductivity produced is very dependent on the individual electron energy: higher energy electrons penetrate deeper into the atmosphere to regions where conductivity production is more efficient. In JIM, it was found that a precipitation flux of ~10mW m^{-2} would be required to produce a value of Σ_P = 1.8mho in the Planetary Reference Frame, if 60 keV electrons were precipitated (the average precipitation energy used in JIM, higher than those proposed in Paper II, which suggests ~20 keV electrons). Allowing the coupling parameter, K (see Cowley and Bunce, 2001, for definition), of the neutral atmosphere to the ions in the polar cap to be ~0.6 - a value that is routinely found for Jupiter (Millward *et al*., 2003) - the value of Σ^*_P = 0.72mho would be produced by ~10mW m^{-2} of 60 keV electrons. JIM predicts that this flux would produce an H_3^+ column density of $5x10^{16}m^{-2}$. However, the above discussion shows that the derived fluxes are highly dependant on the individual electron energy. Thus, in the absence of *in situ* spacecraft information about the electron energy spectrum, flux values can only be model-specific estimates.

Conclusions

This first ever measurement of the H_3^+ wind speeds in Saturn has borne out the prediction of Paper II that the kronian auroral/polar region is much closer to the terrestrial situation than that of Jupiter, at least as far as plasma flow patterns are concerned. It has also shown that it may well be possible to use the measured wind speeds to deduce important information about ionospheric conductivities, reconnection times, magnetotail dimensions and precipitation fluxes, if the results are combined with models, although it is clear that input parameters in these models – solar wind velocity, electron energy, ion-neutral coupling, *etc*. - have a strong bearing on the outcome. With the arrival of the Cassini/Huygens mission to Saturn in July 2004, magnetospheric plasma flows will be measured *in situ* for the first time in two decades. There will be great interest in maximising the return on the mission and decisions as to what gets measured where and when will be of the utmost importance. The results presented here show that ground-based measurements do play an important part in such discussions and in the interpretation of the spacecraft data.

Acknowledgements

It is a pleasure to acknowledge the expert and assiduous assistance of Paul Sears and Dave Griep, telescope operators for the IRTF, in obtaining the data discussed here. We would also like to thank Stan Cowley, Emma Bunce and Renée Prangé for sending us their paper prior to publication, and for their helpful

discussions in preparing this manuscript. The comments of our two referees significantly improved the paper. TS would like to thank the UK Particle Physics and Astronomy Research Council (PPARC) for a research fellowship.

References

Achilleos, N., S. Miller, J. Tennyson, A.D. Aylward, I. Meuller-Wodarg and D. Rees, 1998. JIM: a time-dependent, three-dimensional model of Jupiter's thermosphere and ionosphere. *J. Geophys. Res.* **103**, 20089-20112.

Broadfoot, A.L. and 15 others, 1981. Extreme ultraviolet observations from Voyager 1 encounter with Saturn. *Science* **212**, 206.

Clarke, J.T., H.W. Moos, S.K. Atreya and A.L. Lane, 1981. IUE detection of bursts of H Ly α from Saturn. *Nature* **290**, 226-229.

Cowley, S.W.H. and E.J. Bunce, 2001. Origin of the main auroral oval in Jupiter's coupled magnetosphere-ionosphere system. *Planet. Space Sci.* **49**, 1067-1088.

Cowley, S.W.H., E.J. Bunce, T. Stallard and S. Miller, 2003a. Jupiter's polar ionospheric flows: theoretical interpretation. *Geophys. Res. Lett.* **30**, L24.

Cowley, S.W.H., E.J. Bunce and R. Prangé, 2003b. Saturn's polar ionospheric flows and their relation to the main auroral oval. *Ann. Geophys.*, submitted.

Dungey, J.W., 1961. The interplanetary magnetic field and auroral zones. *Phys. Rev. Lett.* **6**, 47.

Geballe, T.R., M.-F. Jagod and T. Oka, 1993. Detection of H_3^+ emission lines in Saturn. *Astrophys. J.* **410**, L109-L112.

Gurnett, D.A., W.S. Kurth and F.W. Scarf, 1981. Plasma waves near Saturn: initial results from Voyager 1. *Science* **212**, 235.

Greene, T.P., A. T. Tokunaga, D. W. Toomey and J. S. Carr, 1993. CSHELL: A High Spectral Resolution 1 - 5 micron Cryogenic Echelle Spectrograph for the IRTF. *Proc. SPIE* **1946**, 313-321.

Hill, T.W., 1979. Inertial limit on corotation. *J. Geophys. Res.* **84**, 6554-6558.

Hill, T.W. and A.J. Dessler, 1991. Plasma motions in planetary magnetospheres. *Science* **252**, 410-415.

Hill, T.W., 2001. The jovian auroral oval. *J. Geophys. Res.* **106**, 8101-8107.

Judge, D.L., F.M. Wu and R.W. Carlson, 1980. Ultraviolet photometer observations of the Saturnian system. *Science* **207**, 431.

Kaiser, M.L., M.D. Desch, W.S. Kurth, A. Lecacheux, F. Genova, B.M. Pederson and D.R. Evans, 1984. Saturn as a radio source, in *Saturn*, eds. T. Gehrels and

M.S. Matthews (Univ. Arizona Press, Tucson), 378.

Millward G., S. Miller, T. Stallard and A.D. Aylward, 2002. On the dynamics of the jovian thermosphere and ionosphere III: the modelling of auroral conductivity. *Icarus* **160**, 95-107.

Millward G., S. Miller, T. Stallard and A.D. Aylward, 2003. On the dynamics of the jovian thermosphere and ionosphere IV: ion-neutral coupling. *Icarus* submitted.

Rego, D., N. Achilleos, T. Stallard, S. Miller, R. Prangé, M. Dougherty and R.D. Joseph, 1999. Supersonic winds in Jupiter's aurorae. *Nature* **399**, 121-124.

Richardson, J.D., and Sittler, E.C., Jr, 1990. A plasma density model for Saturn based on Voyager observations, *J. Geophys. Res*., **95**, 12019

Sandel, B.R. and A.L. Broadfoot, 1981. Morphology of Saturn's aurora. *Nature* **292**, 679.

Stallard T., S. Miller, G.E. Ballester, D. Rego, R. Joseph and L. Trafton, 1999. The H_3^+ Latitudinal Profile of Saturn. *Ap. J. Lett.,* **521**, L149-152.

Stallard, T., S. Miller, G. Millward and R.D. Joseph, 2001. On the dynamics of the jovian ionosphere and thermosphere II: the measurement of H_3^+ vibrational temperature, column density and total emission. *Icarus* **154**, 475-491.

Stallard, T., S. Miller, S.W.H. Cowley and E.J. Bunce, 2003. Jupiter's polar ionospheric flows: measured intensity and velocity variations poleward of the main auroral oval. *Geophys. Res. Lett.* **30**, L25.

Trafton, L.M., S. Miller, T.R. Geballe, J. Tennyson and G.E. Ballester, 1999. H_2 quadrupole and H_3^+ emission from Uranus: the uranian thermosphere, ionosphere and aurora. *Astrophys. J.* **524**, 1059-1083.

Trauger, J.T. and 16 others, 1998. Saturn's hydrogen aurora: widefield planetary camera 2 imaging from the Hubble Space Telescope. *J. Geophys. Res.* **103**, 20237-20244.

Vasyliunas, V.M., 1983. Plasma distribution and flow, in *Physics of the jovian magnetosphere*, ed. A.J. Dessler (Cambridge University Press), 395-453.